THE JOURNAL OF BIOLOGICAL CHEMISTRY VOL. 286, NO. 29, pp. 26003–26015, July 22, 2011

Wnt/β-Catenin Pathway in Podocytes Integrates Cell Adhesion, Differentiation, and Survival*[S]

Received for publication, January 21, 2011, and in revised form, May 4, 2011 Published, JBC Papers in Press, May 25, 2011, DOI 10.1074/jbc.M111.223164

Hideki Kato[‡], Antje Gruenwald[‡], Jung Hee Suh[§], Jeffrey H. Miner[§], Laura Barisoni-Thomas[¶], Makoto M. Taketo[‖], Christian Faul[**], Sarah E. Millar[‡‡], Lawrence B. Holzman[§§], and Katalin Susztak[‡¶¶1]

From the [‡]Department of Medicine, Division of Nephrology, Albert Einstein College of Medicine, New York, New York 10461, the [§]Renal Division, Department of Internal Medicine, Washington University School of Medicine, St. Louis, Missouri 63110, the [¶]Department of Pathology, New York University School of Medicine, New York, New York 10016, the [‖]Department of Pharmacology, Graduate School of Medicine, Kyoto University, Kyoto 606-8501, Japan, the [**]Department of Medicine, Division of Nephrology, Miller School of Medicine, University of Miami, Coral Gables, Florida 33136, the [‡‡]Department of Dermatology, University of Pennsylvania School of Medicine, Philadelphia, Pennsylvania 19104-6100, the [§§]Department of Medicine, Renal, Electrolyte, and Hypertension Division, University of Pennsylvania School of Medicine, Philadelphia, Pennsylvania 19104, and the [¶¶]Department of Genetics, Albert Einstein College of Medicine, Bronx, New York 10461

Diabetic kidney disease (DKD) is the single most common cause of albuminuria and end-stage kidney disease in the United States. We found increased expression of Wnt/β-catenin (Ctnnb1) pathway transcripts and proteins in glomeruli and podocytes of patients and mouse models of DKD. Mice with podocyte-specific expression of stabilized Ctnnb1 exhibited basement membrane abnormalities, albuminuria, and increased susceptibility to glomerular injury. Mice with podocyte-specific deletion of Ctnnb1 or podocyte-specific expression of the canonical Wnt inhibitor Dickkopf-related protein 1 (Dkk1) also showed increased susceptibility to DKD. Podocytes with stabilized Ctnnb1 were less motile and less adhesive to different matrices. Deletion of Ctnnb1 in cultured podocytes increased the expression of podocyte differentiation markers and enhanced cell motility; however, these cells were more susceptible to apoptosis. These results indicate that Wnt/Ctnnb1 signaling in podocytes plays a critical role in integrating cell adhesion, motility, cell death, and differentiation. Balanced Ctnnb1 expression is critical for glomerular filtration barrier maintenance.

Diabetic kidney disease (DKD)[2] is one of the most devastating complications of diabetes and the single most common cause of albuminuria, chronic kidney disease, and end-stage renal disease (ESRD) in the Western world (1). DKD causes filtration unit dysfunction leading to the development of albuminuria, which is the most abundant protein component of the blood. The glomerular filtration barrier consists of three layers as follows: glomerular endothelial cells, the glomerular basement membrane (GBM), and the glomerular epithelial cell (or podocyte) layer (2–4). Decreased glomerular podocyte density is shown to be the strongest predictor for end-stage renal disease development in patients with diabetes (5). Hyperglycemia via the generation of reactive oxygen species induces podocyte apoptosis and loss, which has been well documented in many different mouse DKD models (6, 7). As podocytes are terminally differentiated cells, they are unable to proliferate; therefore, apoptosis or detachment can lead to podocyte deficiency, which in turn will lead to glomerulosclerosis development (8, 9). Early administration of drugs that prevent podocyte apoptosis has been shown to ameliorate DKD in rodent models; however, this may not be a clinically translatable strategy (6, 10). Another early lesion in diabetes is the thickening of the basement membrane. The role and mechanism of GBM thickening are not fully understood. It is speculated that GBM thickening could cause alterations in integrin expression, which could interfere with podocyte adhesiveness. Genetic deletion of podocyte-specific integrins, Itgb1 and Itga3, causes albuminuria and glomerulosclerosis; however, the contribution of podocyte adhesion to DKD development has not been demonstrated (11, 12). Understanding the mechanism of podocyte differentiation, adhesion and cell death could be highly relevant for the development of targets for intervention.

β-Catenin (Ctnnb1) is a multifunctional protein; it plays a key role in cell adhesion; in addition, it regulates Wnt-mediated transcription. In the absence of Wnt ligand, β-catenin is targeted for degradation via phosphorylation of its serine (Ser-33/34/45) and threonine (Thr-41) sites by glycogen synthase kinase-3β (GSK-3β) (13). Upon ligand binding, inhibition of GSK-3β stabilizes Ctnnb1, leading to its cytoplasmic accumulation and subsequent nuclear translocation (14). In the nucleus, Ctnnb1 binds to lymphocyte enhancer factor-1/T cell factor transcription factors to mediate gene transcription. Genome-wide association studies indicate a correlation between *TCF7L2* (also known as *TCF-4*) polymorphism and the development of diabetes, chronic kidney disease, and DKD (15, 16). Recent genome-wide transcript profiling studies by Cohen

* This work was supported, in whole or in part, by National Institutes of Health Grants 5R01DK076077-04 (to K. S.) and R01DK078314 (to J. H. M.). This work was also supported by the American Diabetes Association (to K. S.), the NephCure Foundation, and the Uehara Memorial Foundation (to H. K.).

[S] The on-line version of this article (available at http://www.jbc.org) contains supplemental Figs. 1–6 and Tables 1–4.

[1] To whom correspondence should be addressed: Division of Nephrology, Albert Einstein College of Medicine, 1300 Morris Park Ave., Bronx, NY 10461. Tel.: 718-430-3498; Fax: 718-430-8963; E-mail: katalin.susztak@einstein.yu.edu.

[2] The abbreviations used are: DKD, diabetic kidney disease; GBM, glomerular basement membrane; BIO, 2′*Z*,3′*E*)-6-bromoindirubin-3′-acetoxime; STZ, streptozotocin; QRT, quantitative real-time; TDZD-8, 4-benzyl-2-methyl-1,2,4-thiadiazolidine-3,5-dione; TEM, transmission EM; PAS, periodic acid-Schiff.

et al. (17) found increased Wnt mRNA levels in the tubulointerstitial compartment of kidney biopsy samples obtained from patients with DKD. Studies from Dai *et al.* (18) reported increased Wnt/Ctnnb1 activity in an acute high dose adriamycin-induced proteinuria model. They proposed that the Wnt/Ctnnb1 pathway directly causes podocyte damage via inducing podocyte epithelial-mesenchymal transition and down-regulation of Snail and nephrin. In contrast, Lin *et al.* (19) suggested that hyperglycemia and diabetes cause down-regulation of *Wnt4* and *Wnt5a* and decreased Ctnnb1 nuclear translocation in murine glomerular mesangial cells. They also proposed that sustaining Wnt/Ctnnb1 signaling is beneficial for promoting survival of high glucose-stressed cells and protects mice from DKD (20). These contradictory results highlight the importance of the use of *in vivo* cell type-specific transgenic animals to define the role of the Wnt/Ctnnb1 pathway in the glomerulus.

Here, we analyzed the role of the Wnt/Ctnnb1 pathway in podocytes at base line and in DKD. *In vitro* and *in vivo* studies indicated that Wnt/Ctnnb1 pathway plays a key role in determining podocyte differentiation, motility, cell-matrix adhesion, and cell death.

EXPERIMENTAL PROCEDURES

Human Kidney Samples—Human kidney samples were collected from kidney biopsies and nephrectomies. The study was approved by the Institutional Board Review. The biopsy tissue was manually microdissected at 4 °C in RNALater as described previously (21).

Microarray Studies—Microarray studies on isolated human kidney glomeruli were performed as described previously (21). Affymetrix U133Av2 chips were used to hybridize human samples. Mouse glomeruli were isolated using the magnetic bead method (22), and Affymetrix 1.0 ST arrays were used for gene expression analysis. Data normalization, storage, and statistical analyses were performed using GeneSpring GX software version 10.0 (Agilent Technologies, Palo Alto, CA) with the gcRMA method (21).

Animals—Genotypes were identified by genomic PCR analysis using published allele-specific primers (primer list is available upon request). To generate mice with podocyte-specific stabilized Ctnnb1 expression, mice in which exon3 of Ctnnb1 is floxed ($Ctnnb1^{FloxE3/FloxE3}$) (23) were crossed with transgenic mice expressing Cre recombinase under the control of the podocin promoter ($NPHS2^{Cre}$ mice) (24). $NPHS2^{Cre}$/$Ctnnb1^{FloxE3/WT}$, $NPHS2^{Cre}$/$Ctnnb1^{FloxE3/FloxE3}$, and WT/$Ctnnb1^{FloxE3/WT}$ or WT/$Ctnnb1^{FloxE3/FloxE3}$ (control) male littermates were used for the experiments. To generate podocyte-specific Ctnnb1 knock-out mice (intron1–6 floxed), $Ctnnb1^{KO/KO}$ mice (25) were crossed with $NPHS2^{Cre}$ mice, and $NPHS2^{Cre}$/$Ctnnb1^{KO/KO}$ and WT/$Ctnnb1^{KO/KO}$ (control) male littermates were used for the experiments. To generate podocyte-specific inducible Dickkopf-related protein 1 (Dkk1) mice, we crossed podocyte-specific reverse tTA (rtTA)-expressing mice ($NPHS2^{rtTA}$) (26) with the mice carrying the *tetO* promoter linked to Dkk1 (TRE-Dkk1) transgenic mice (27). Single transgenic $NPHS2^{rtTA}$ and TRE-Dkk1 littermates were used as controls. Animals were placed on doxycycline-containing food starting at 3 weeks of age. For the diabetic nephropathy model, uninephrectomy was performed on 4-week-old male mice under sterile conditions. Animals were injected with STZ (50 mg/kg intraperitoneally for five days, low dose protocol) as detailed on line. Mice were sacrificed at 20 weeks of age. To reduce heterogeneity, only male mice were used in our experiments. All animal studies were approved by the Animal Care Committee, Albert Einstein College of Medicine. Animals were maintained under specific pathogen-free conditions.

Renal Phenotype Analysis—Urinary albumin and creatinine were determined using mouse albumin-specific ELISA and creatinine companion kits (Exocell and Bethyl Laboratories). Renal histological analysis was performed on formalin-fixed paraffin-embedded kidney sections stained with periodic acid-Schiff (PAS). GBM thickness was determined by the orthogonal intercept method as described previously (28, 29). Podocyte number was estimated on 4-μm paraffin sections stained with Wt1 (M3561, DAKO).

Immunostaining—Immunofluorescence studies were performed on optimal tissue cutting compound-embedded frozen kidney sections as described earlier (10). The complete list of primary and secondary antibodies used for the experiments are listed in supplemental Table 3. Staining was visualized using fluorescent secondary antibodies or peroxidase-conjugated anti-rabbit or anti-mouse Vectastain Elite kit and diaminobenzidine (DAB) (Vector Laboratories). Terminal dUTP labeling (TUNEL) staining was performed using the TUNEL kit (Chemicon).

Podocyte Cell Culture Experiment—Podocyte cell lines were established as described previously from Immorto mice (30). To induce Cre-mediated recombination, podocytes (at 30–50% confluent level) were infected with Cre or control adenovirus (Cell Biolabs, Inc.) at a multiplicity of infection of 50 in 6-well plates.

Migration Assay—Migration assay was performed as described previously (31). In brief, cells were cultured on type I collagen-coated 6-well plates to become confluent. Cells were growth-arrested in 0.2% FBS for 12 h and then scratched with a 200-μl pipette tip. Cells were treated with PBS (control), LiCl (20 mM, Sigma), 4-benzyl-2-methyl-1,2,4-thiadiazolidine-3,5-dione (TDZD-8) (3 μM, Calbiochem), or (2′*Z*,3′*E*)-6-bromoindirubin-3′-acetoxime (BIO) (30 nM, Calbiochem). After 24 h, more than 64 images were taken from scratched areas, and the number of migrated cells was counted. Three independent experiments were performed.

Adhesion Assay—Adhesion assays were performed using the Vybant cell adhesion assay (Invitrogen) according to the manufacturer's instructions (31). Four days after Cre or control adenoviral infection, cells were harvested and incubated with calcein AM for 30 min. Single cell podocyte suspensions were plated on collagen type I, IV, or laminin-coated 96-well plates (1×10^5 cells/well). Cells were washed four times with PBS. The amount of adherent cells was determined by absorbance of 485 nm and emission of 535 nm. LiCl, TDZD-8, thiadiazolidine-3,5-dione, BIO (concentrations are the same as above), or 50 ng/ml mouse recombinant Wnt3a (R & D Systems) were used in the adhesion assays. The assay was normalized to 100% FCS- and 1% BSA-coated plates. The difference of the 100% FCS and 1% BSA was set as 100%, and the data are expressed as percent of this control. Three independent experiments were performed.

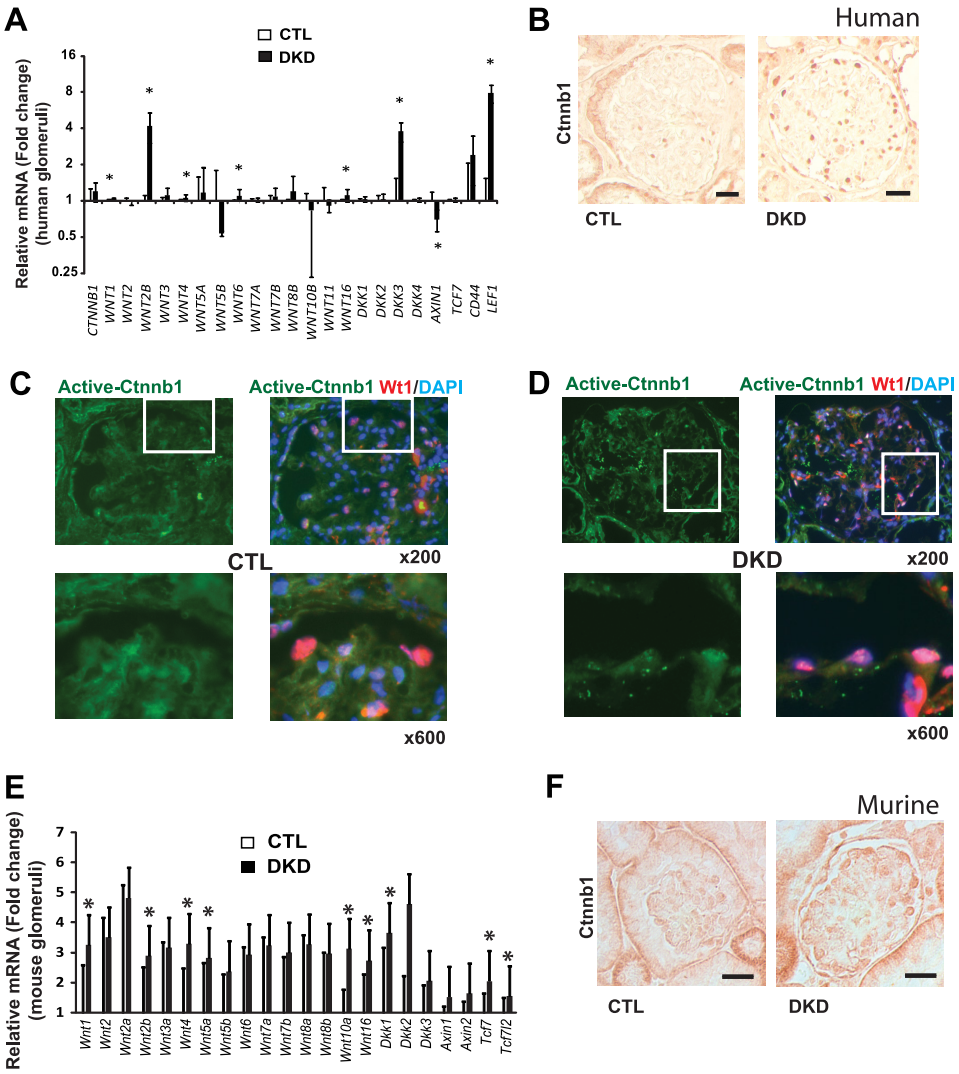

FIGURE 1. **Increased podocyte Wnt/Ctnnb1 signaling in patients and mice with diabetic kidney disease.** *A*, relative mRNA levels in control (*CTL*) and DKD. The *y* axis is the logarithmic scale of fold change values as compared with the average of control groups, and the data represent means ± S.D. *, $p < 0.05$. *B*, immunostainings for total Ctnnb1 of human healthy (*CTL*) and DKD glomeruli. *Scale bar*, 40 μm. *C* and *D*, immunofluorescent co-stainings of active Ctnnb1 (*green*) and podocyte marker Wt1 (*red*) in control and DKD of human kidney samples with DAPI (*blue*) nuclear counterstaining. *E*, gene expression changes in isolated glomeruli of control (*CTL*) and STZ-treated diabetic kidneys (DKD, *black bars*). The *y* axis is the fold change values as compared with the average of control groups, and the data represent means ± S.D. *, $p < 0.05$. *F*, immunostaining for total Ctnnb1 in control and diabetic mouse kidney samples. *Scale bar*, 20 μm.

Western Blot Analysis—Western blotting was performed as described previously (10). We used the following primary antibodies for the experiments: total Ctnnb1 (sc-7199 Santa Cruz Biotechnology); active Ctnnb1 (05-665, Millipore); and β-actin (ab8226, Abcam). For Wt1 detection of urinary cells, spot urine was collected and centrifuged, and the sediment was dissolved in loading buffer (32).

Quantitative Real Time PCR—Quantitative real time PCR was performed as described earlier (10). The supplemental Table 4 contains the primer sequences used in this study.

Statistical Analysis—Results are presented as mean ± S.D. Student *t* test was used to analyze the difference between two groups. Values were regarded significant at $p < 0.05$.

RESULTS

Activation of the Canonical Wnt/Ctnnb1 Signaling in Patients and Mouse Models of DKD—First we analyzed the following expression, Wnt pathway-related genes in healthy and DKD glomeruli. Demographics of the research participants (supplemental Table 1) indicated similar age and body mass between control and DKD groups. DKD patients presented with advanced (stage III–V) chronic kidney disease. Gene expression arrays were performed using the Affymetrix U133Av2.0 chips on microdissected human glomeruli obtained from healthy (control, $n = 12$) individuals and DKD patients ($n = 7$). Our analysis indicated a statistically significant increase in mRNA expression of *WNT1*, *WNT2B*, *WNT4*, *WNT6*, *WNT16*, *DKK3*, and *Lef1* (Fig. 1*A*) in human DKD glomeruli. Expression of Wnt/Ctnnb1 target gene *LEF1* was significantly increased in DKD glomeruli, indicating the transcriptional activation of the pathway. In human DKD kidney samples, there was an increase in Ctnnb1 immunostaining in glomeruli as compared with healthy control kidneys (Fig. 1*B*). Detailed study to determine the localization of Ctnnb1 by immunofluorescent co-stainings for Ctnnb1 and the podocyte marker Wt1 indicated

increased Ctnnb1 expression in podocytes (Fig. 1, *C* and *D*).

We also detected a statistically significant increase in mRNA levels for *Wnt1*, *Wnt2b*, *Wnt4*, *Wnt5a*, *Wnt10a*, *Wnt16*, *Dkk1*, *Tcf7*, and *Tcf7l2* (Fig. 1*E*) in glomeruli of 20-week-old STZ-treated diabetic mice when compared with controls. Likewise, immunostaining experiments showed increased expression of Ctnnb1 in diabetic mouse glomeruli (Fig. 1*F*). These results indicate increased Wnt/Ctnnb1 signaling in glomeruli and increased nuclear Ctnnb1 expression in podocyte in patients and mouse models of DKD.

Podocyte-specific Expression of Stabilized Ctnnb1 in Vivo Leads to GBM Thickening, Albuminuria, and Glomerulosclerosis Features of DKD—To determine whether the Wnt/Ctnnb1 pathway plays a functional role *in vivo* in podocytes, we expressed stabilized Ctnnb1 by intercrossing Podocin-Cre ($NPHS2^{Cre}$) mice (24) with mice in which the third exon of Ctnnb1 is flanked by LoxP sites ($Ctnnb1^{FloxE3}$) (23). Exon3 of Ctnnb1 contains serine/threonine residues that are key targets of phosphorylation. By deleting the phosphorylation site, Ctnnb1 is rendered into a stabilized and dominant active form. The strategy to generate heterozygous, homozygous, and control mice is described in supplemental Fig. 6. We confirmed increased expression of Ctnnb1 specifically in podocytes of $NPHS2^{Cre}/Ctnnb1^{FloxE3/WT}$ mice (Fig. 2*A*). Immunoblot analysis of isolated glomeruli confirmed the expression of the mutant (exon3 deleted) lower molecular weight band of Δexon3 Ctnnb1 (Fig. 2*B*).

Renal histology examined by PAS staining showed mild mesangial expansion in 20-week-old $NPHS2^{Cre}/Ctnnb1^{FloxE3/WT}$ mice (Fig. 2*C*). Transmission electron microscopy studies of $NPHS2^{Cre}/Ctnnb1^{FloxE3/WT}$ mice showed diffuse global thickening of the GBM (Fig. 2*D*). GBM abnormalities were evident as early as 4 weeks of age and became progressively severe by 20 weeks (Fig. 2*D*). Podocyte foot processes appeared normal with occasional effacement, which was prominent in areas of severe GBM change. Age-matched $NPHS2^{Cre}$ or $Ctnnb1^{FloxE3/WT}$ littermates (used as controls in this study) showed no GBM changes. $NPHS2^{Cre}/Ctnnb1^{FloxE3/WT}$ mice developed significant albuminuria beginning at around 10 weeks of age (Fig. 2*E*). In summary, mice with podocyte-specific expression of stabilized Ctnnb1 showed early GBM alterations followed by later development of albuminuria, a phenotype akin to that of early DKD in patients.

Next, we examined the effect of diabetes in the $NPHS2^{Cre}/Ctnnb1^{FloxE3/WT}$ mice. We induced type 1 diabetes in uninephrectomized male mice with a low dose STZ injection (at 5 weeks of age) (33). Albuminuria was highly increased in diabetic $NPHS2^{Cre}/Ctnnb1^{FloxE3/WT}$ mice compared with control mice (Fig. 2*F*). In addition, $NPHS2^{Cre}/Ctnnb1^{FloxE3/WT}$ diabetic mice developed significant glomerulosclerosis (Fig. 2*G*), which was not evident in control mice nor in nondiabetic $NPHS2^{Cre}/Ctnnb1^{FloxE3/WT}$ animals. These results suggest the higher susceptibility to diabetic injury in the $NPHS2^{Cre}/Ctnnb1^{FloxE3/WT}$ mice.

Mice homozygous for the stabilized Ctnnb1 ($NPHS2^{Cre}/Ctnnb1^{FloxE3/FloxE3}$) allele showed severe albuminuria and glomerulosclerosis already at 8 weeks of age (Fig. 2, *H* and *I*). Electron microscopy analysis of the $NPHS2^{Cre}/Ctnnb1^{FloxE3/FloxE3}$ mice was consistent with severe GBM thickening (Fig. 2*J*). Our results indicate that enhanced Ctnnb1 activity in podocytes causes a change in GBM morphology and increases susceptibility to diabetic kidney injury.

Unraveling Ctnnb1-induced GBM Changes—To understand Ctnnb1-induced GBM changes, first we performed detailed morphometric quantification of the GBM width. GBM width was almost double in 8-week-old $NPHS2^{Cre}/Ctnnb1^{FloxE3/WT}$ mice compared with controls (120.0 ± 15.6 *versus* 225.2 ± 42.1 nm) (Fig. 3*A*). The difference in GBM thickness remained significant at 20 weeks of age (169.3 ± 17.7 *versus* 325.6 ± 4.7 nm) (Fig. 3*B*), but the degree of difference (about 2-fold) did not increase when compared with control mice, despite the fact that the animals developed albuminuria during this period. The GBM width of 8-week-old male $NPHS2^{Cre}/Ctnnb1^{FloxE3/WT}$ mice (with mild albuminuria) and 8-week-old $NPHS2^{Cre}/Ctnnb1^{FloxE3/FloxE3}$ mice (with severe albuminuria and glomerulosclerosis) showed no statistical difference (225.2 ± 42.1 *versus* 276.1 ± 26.3 nm) (Fig. 3*C*).

Disruption of the ability of GBM to act as a charge barrier is considered one of the causes of albuminuria (34). Therefore, we used electron microscopic analysis to examine GBM anionic charge sites labeled by the cationic probe polyethyleneimine (supplemental Fig. S1*A*). Quantification of polyethyleneimine aggregate density in the GBM did not a show significant difference in subepithelial and subendothelial anionic sites as compared with control mice (supplemental Fig. S1*B*). These experiments failed to show a correlation between GBM thickening or change selectivity and albuminuria and glomerulosclerosis in mice with podocyte-specific stabilized Ctnnb1 expression.

Quantitative real time-PCR (QRT-PCR)-based transcript studies of isolated glomeruli indicated an increase in *Col4a2* and *Col4a5* expressions in 8-week-old $NPHS2^{Cre}/Ctnnb1^{FloxE3/WT}$ mice (Fig. 3*D*). At 20 weeks of age, we observed increased transcript levels of *Col4a1,6* in addition to the *Col4a2,5* isoforms (Fig. 3*E*). Similarly, in 8-week-old homozygous $NPHS2^{Cre}/Ctnnb1^{FloxE3/FloxE3}$ mice, *Col4a1, -2,* and *-6* isoforms were increased (Fig. 3*F*). Immunofluorescence studies confirmed the increased Col4a2 and Lamb1 expression in $NPHS2^{Cre}/Ctnnb1^{FloxE3/WT}$ mice (Fig. 3, *G* and *H*). Col4a2 and Lamb1 were mainly expressed in the mesangial area in control animals. In $NPHS2^{Cre}/Ctnnb1^{FloxE3/WT}$ mice, in addition to the mesangial expression of Col4a2 and Lamb1, there was also more prominent staining in the capillary loops. Similar results were noted in the $NPHS2^{Cre}/Ctnnb1^{FloxE3/FloxE3}$ mice (supplemental Fig. S2). These results suggest that the GBM of $NPHS2^{Cre}/Ctnnb1^{FloxE3/WT}$ mice constitutes overproduction of collagens mostly observed in mesangial and parietal basement membrane (*Col4a1, -2, -5,* and *-6*), which is similar to what is observed in patients with DKD (34, 35).

Next, we analyzed the expression levels of matrix metalloproteinases, which affect the turnover and breakdown of extracellular matrix and glomerulus. In 8-week-old $NPHS2^{Cre}/Ctnnb1^{FloxE3/WT}$ mice, transcript levels of *Mmp7* and *Mmp16* were significantly decreased, whereas *Mmp2* expression was increased already at 8 weeks of age (Fig. 3*I*). At 20 weeks of age, there was a significant increase in *Mmp14* and *Mmp23* expres-

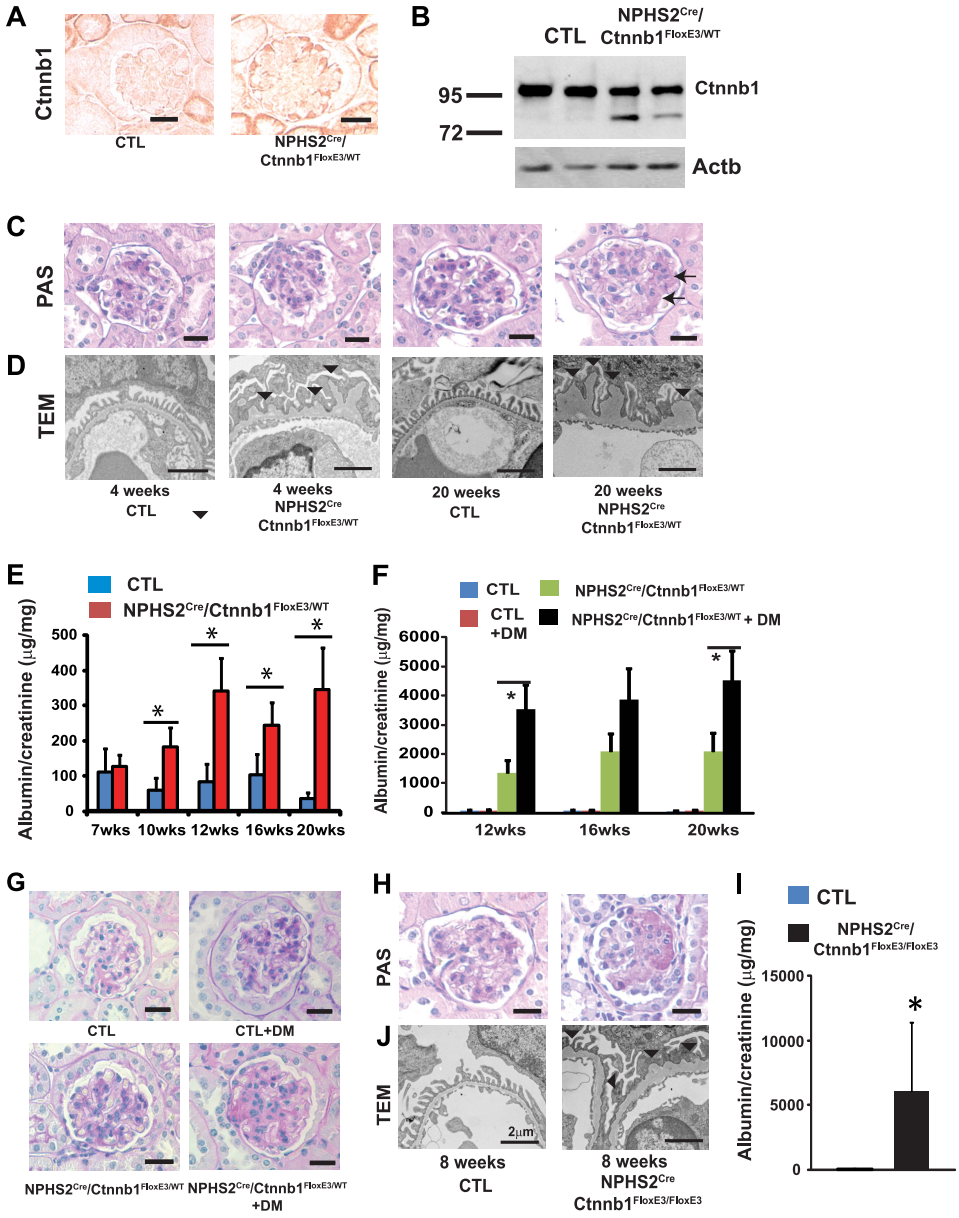

FIGURE 2. **Podocyte-specific stabilized Ctnnb1 expression induces GBM alterations and albuminuria and enhances the susceptibility for diabetic injury.** *A*, total Ctnnb1 immunostaining in 8-week-old control (*CTL*) and NPHS2^{Cre}/Ctnnb1$^{FloxE3/WT}$ mice. *B*, Ctnnb1 and β-actin (*Actb*) Western blots of isolated glomeruli from control and NPHS2^{Cre}/Ctnnb1$^{FloxE3/WT}$ mice. Note the lower molecular weight delta-exon3 Ctnnb1 band of NPHS2^{Cre}/Ctnnb1$^{FloxE3/WT}$ mice. *C*, PAS staining; *D*, TEM image of kidney sections from control and NPHS2^{Cre}/Ctnnb1$^{FloxE3/WT}$ mice. *Arrow* and *arrowhead* indicate the mild mesangial expansion (*C*) and thickening of GBM (*D*), respectively. *E*, albumin-to-creatinine ratios (μg/mg) of spot urine samples of control (*CTL*; *blue bars*) and NPHS2^{Cre}/Ctnnb1$^{FloxE3/WT}$ mice ($n = 10$ mice per group). *F*, albumin-to-creatinine ratios of spot urine samples of control (*CTL*), control diabetic (*CTL+DM*), NPHS2^{Cre}/Ctnnb1$^{FloxE3/WT}$, and diabetic NPHS2^{Cre}/Ctnnb1$^{FloxE3/WT}$ mice ($n = 7$ mice per group). *G*, PAS staining of 20-week-old control (*CTL*), control diabetic (*CTL+DM*), NPHS2^{Cre}/Ctnnb1$^{FloxE3/WT}$, and diabetic NPHS2^{Cre}/Ctnnb1$^{FloxE3/WT}$ mice. Diabetic NPHS2^{Cre}/Ctnnb1$^{FloxE3/WT}$ mice showed mild glomerulosclerosis. *H*, PAS-stained 8-week-old control (*CTL*) and homozygous NPHS2^{Cre}/Ctnnb1$^{FloxE3/FloxE3}$ mice (*right*). *Scale bar*, 20 μm. *I*, albumin-to-creatinine ratio of 8-week-old control (*CTL*, *left*) and NPHS2^{Cre}/Ctnnb1$^{FloxE3/FloxE3}$ mice (*right*) ($n = 7$ per group). *J*, TEM images of control and NPHS2^{Cre}/Ctnnb1$^{FloxE3/FloxE3}$ mice. *Scale bar*, 2 μm.

sion (Fig. 3*J*). These most likely indicate an alteration in GBM remodeling in NPHS2^{Cre}/Ctnnb1$^{FloxE3/WT}$ mice. In summary, we found no clear linear correlation between basement membrane width and negative charge barrier selectivity and albuminuria development in NPHS2^{Cre}/Ctnnb1$^{FloxE3/WT}$ mice. We detected alterations in GBM turnover and overall composition shifting from Col4a3 and -4 to Col4a1, -2, -5, and -6.

Ctnnb1 Activation Induces Podocyte Detachment and Loss—To further understand the mechanism of albuminuria and glomerulosclerosis in NPHS2^{Cre}/Ctnnb1$^{FloxE3/FloxE3}$ mice, we performed transcriptome analysis using mouse 1.0 ST Affymetrix gene expression arrays (36). Glomeruli were isolated from 20-week-old control and NPHS2^{Cre}/Ctnnb1$^{FloxE3/WT}$ mice ($n = 3$) as well as 8-week-old control and NPHS2^{Cre}/Ctnnb1$^{FloxE3/FloxE3}$ mice ($n = 3$). Analysis of variance identified 2095 probes with statistically significant differential expression; the complete list of differentially expressed probes can be found in supplemental Table 2.

Gene expression analysis indicated a significant decrease in mRNA levels of podocyte-specific genes *Nphs2*, *Wt1*, *Synpo*,

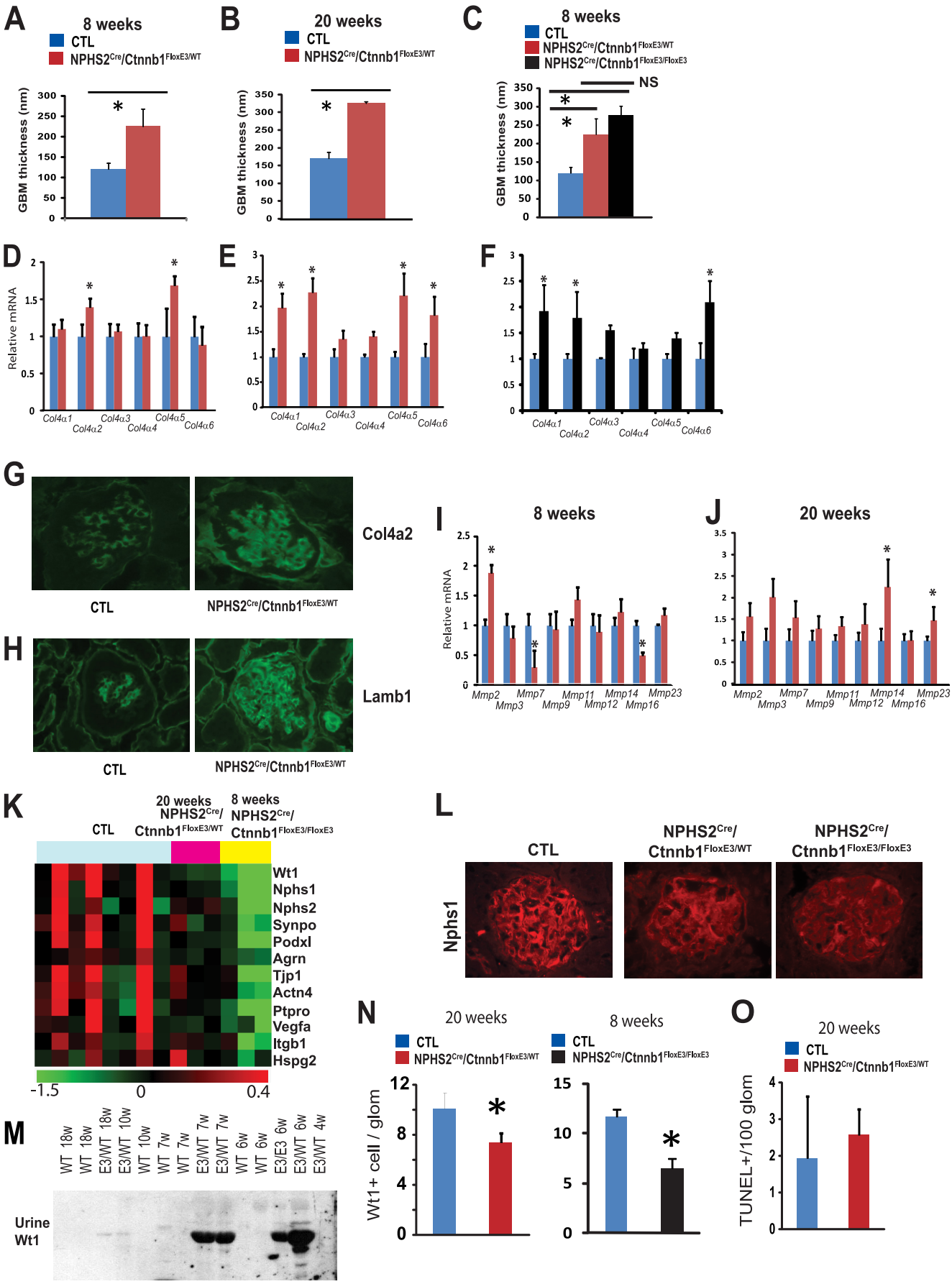
A
8 weeks
CTL
NPHS2Cre/Ctnnb1FloxE3/WT
GBM thickness (nm)
B
20 weeks
CTL
NPHS2Cre/Ctnnb1FloxE3/WT
GBM thickness (nm)
C
8 weeks
CTL
NPHS2Cre/Ctnnb1FloxE3/WT
NPHS2Cre/Ctnnb1FloxE3/FloxE3
NS
GBM thickness (nm)
D
Relative mRNA
Col4α1
Col4α2
Col4α3
Col4α4
Col4α5
Col4α6
E
F
G
Col4a2
CTL
NPHS2Cre/Ctnnb1FloxE3/WT
H
Lamb1
CTL
NPHS2Cre/Ctnnb1FloxE3/WT
I
8 weeks
Relative mRNA
Mmp2
Mmp3
Mmp7
Mmp9
Mmp11
Mmp12
Mmp14
Mmp16
Mmp23
J
20 weeks
K
CTL
20 weeks NPHS2Cre/ Ctnnb1FloxE3/WT
8 weeks NPHS2Cre/ Ctnnb1FloxE3/FloxE3
Wt1
Nphs1
Nphs2
Synpo
Podxl
Agrn
Tjp1
Actn4
Ptpro
Vegfa
Itgb1
Hspg2
-1.5
0
0.4
L
CTL
NPHS2Cre/ Ctnnb1FloxE3/WT
NPHS2Cre/ Ctnnb1FloxE3/FloxE3
Nphs1
M
WT 18w
WT 18w
E3/WT 18w
E3/WT 10w
WT 10w
WT 7w
WT 7w
E3/WT 7w
E3/WT 7w
WT 6w
WT 6w
E3/E3 6w
E3/WT 6w
E3/WT 4w
Urine Wt1
N
20 weeks
CTL
NPHS2Cre/Ctnnb1FloxE3/WT
Wt1+ cell / glom
8 weeks
CTL
NPHS2Cre/Ctnnb1FloxE3/FloxE3
O
20 weeks
CTL
NPHS2Cre/Ctnnb1FloxE3/WT
TUNEL+/100 glom

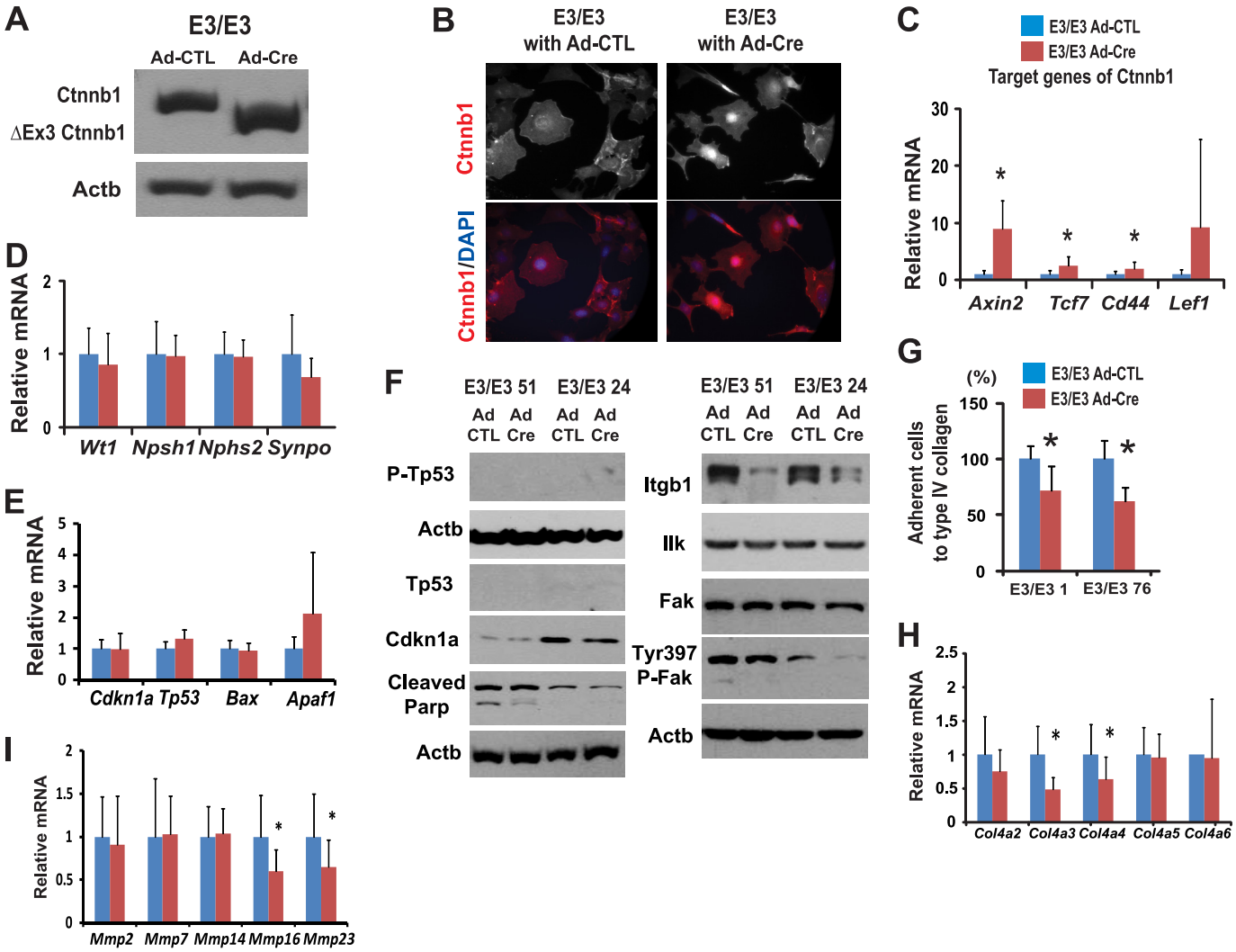

FIGURE 4. **Wnt/Ctnnb1 pathway in podocytes regulates adhesion and migration.** *A,* Western blot for Ctnnb1 of Immorto/Ctnnb1$^{FloxE3/FloxE3}$ podocyte clones (labeled as *E3/E3*) 4 days after control or Cre adenoviral infection. *B,* total Ctnnb1 (*red*) immunocytochemistry of Ctnnb1$^{FloxE3/FloxE3}$ podocytes infected with control (*left*) or Cre adenovirus (*right*). DAPI (*blue*), nuclear counterstaining. *C–E, H,* and *I,* QRT-PCR and Western blot (*F*) analysis of Immorto/Ctnnb1$^{FloxE3/FloxE3}$ clones (E3/E3) infected with control or Cre adenovirus. QRT-PCR data are expressed as mean fold change ± S.D. Paired *t* test was used for QRT-PCR, *, $p < 0.05$. *G,* podocyte adhesion to type IV collagen using the Vybant adhesion assay of two independent Ctnnb1$^{FloxE3/FloxE3}$ podocytes clones. The percentage adhesion was calculated relative to that of control adenovirus. *, $p < 0.05$.

Glepp1 (*Ptpro*), and *Pdxl* (Fig. 3*K*) in heterozygous NPHS2^{Cre}/Ctnnb1$^{FloxE3/WT}$ mice, and it was more severe in homozygous NPHS2^{Cre}/Ctnnb1$^{FloxE3/FloxE3}$ animals. Immunofluorescence studies confirmed the decreased expression of Nphs1 in mice with podocyte-specific Ctnnb1 expression (Fig. 3*L*). Wt1-positive podocyte cell number (per glomerular cross-section) was significantly decreased in 20-week-old NPHS2^{Cre}/Ctnnb1$^{FloxE3/WT}$ mice and to an even greater degree in 8-week-old NPHS2^{Cre}/Ctnnb1$^{FloxE3/FloexE3}$ mice, indicating podocyte loss in these animals (Fig. 3*N*). Upon studying the potential cause of podocyte depletion, we did not detect significant differences in the number of TUNEL-positive cells (Fig. 3*O*) or in the expression of apoptosis-associated transcripts (*Tp53, p21, Apaf,* and *Bax*) in NPHS2^{Cre}/Ctnnb1$^{FloxE3/WT}$ mice (supplemental Table S2), nor did we observe any change in the number of Ki67-positive podocytes, a marker for proliferation. When we analyzed urinary Wt1 levels as a marker for urinary podocyte loss and podocyte detachment, we found a significant

FIGURE 3. **Glomerular basement membrane and podocyte alterations in mice with podocyte-specific stabilized Ctnnb1 expression.** *A–C,* quantification of the basement membrane thickness of 8-week-old (*A*) and 20-week-old male (*B*) control (*CTL*) and NPHS2^{Cre}/Ctnnb1$^{FloxE3/WT}$ mice and 8-week-old NPHS2^{Cre}/Ctnnb1$^{FloxE3/FloxE3}$ mice (*C*). *D–F, I,* and *J,* gene expression analysis of isolated glomeruli of 8-week-old (*D* and *I*) and 20-week-old control and NPHS2^{Cre}/Ctnnb1$^{FloxE3/WT}$ mice (*E* and *J*), and 8-week-old control and NPHS2^{Cre}/Ctnnb1$^{FloxE3/FloxE3}$ mice (*F*). Data are expressed as mean fold change ± S.D. *, $p < 0.05$. *G* and *H,* Col4a2 and Lamb1 immunostainings of 20-week-old control and NPHS2^{Cre}/Ctnnb1$^{FloxE3/WT}$ mice. *K,* heat map showing the relative expression levels of podocyte marker genes in control (*CTL*), 20-week-old heterozygous NPHS2^{Cre}/Ctnnb1$^{FloxE3/WT}$, and 8-week-old homozygous NPHS2^{Cre}/Ctnnb1$^{FloxE3/FloxE3}$ mice. *Red* indicates increase of mRNA levels, and *green* indicates decrease in the mRNA levels. Each *row* represents the expression of one probe, and each *column* represents isolated glomeruli from a single animal. *L,* Nphs1 immunostaining of control, NPHS2^{Cre}/Ctnnb1$^{FloxE3/WT}$, and NPHS2^{Cre}/Ctnnb1$^{FloxE3/FloxE3}$ mice. *M,* Western blot analysis for Wt1 of urine lysates of wild type and NPHS2^{Cre}/Ctnnb1$^{FloxE3/WT}$ mice. *N,* Wt1-positive cells per glomeruli in 20-week-old control (*CTL*), NPHS2^{Cre}/Ctnnb1$^{FloxE3/WT}$ mice, 8-week-old control (*CTL*), and NPHS2^{Cre}/Ctnnb1$^{FloxE3/FloxE3}$ mice. *O,* number of TUNEL-positive cells per 100 glomerular cross-sections ($n = 9$ per group).

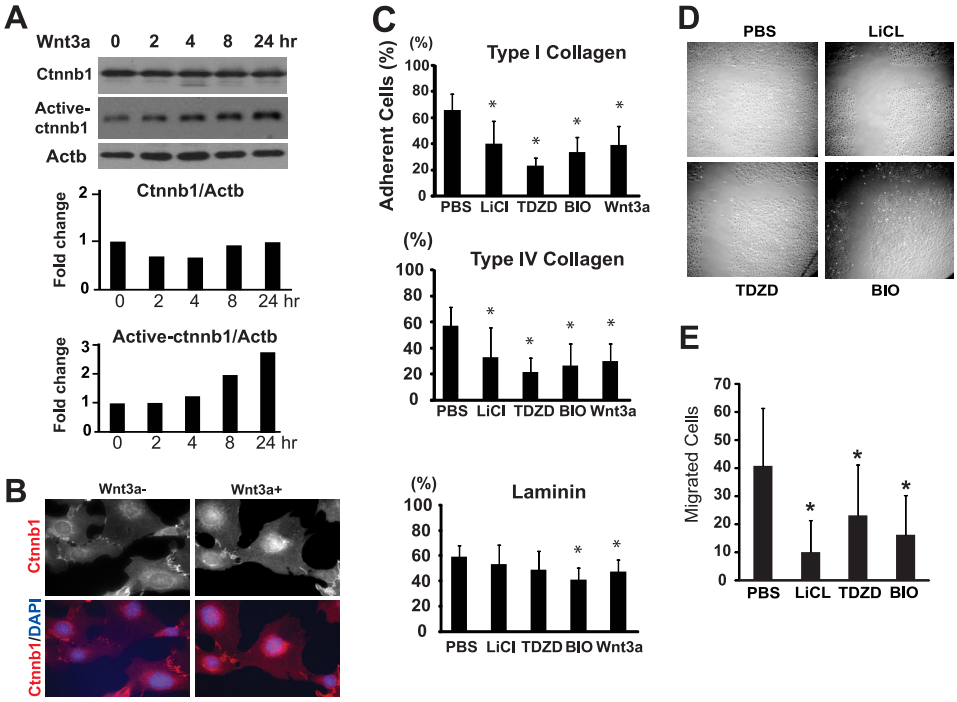

FIGURE 5. **Pharmacological activation of Ctnnb1 decreased cell adhesion and migration.** *A,* Western blot analysis of total and active Ctnnb1 of cultured podocytes incubated with 40 ng/ml recombinant murine Wnt3a. *Lower graphs* show the results of quantification analysis of the expression normalized against β-actin. *B,* podocyte immunostaining of total Ctnnb1 with control PBS (*Wnt3a*−) and Wnt3a stimulation for 24 h. DAPI (*blue*), nuclear counterstaining. *C,* podocyte adhesion to type I and type IV collagen and laminin after the treatment with PBS, 20 mM lithium, 3 μM TDZD, 30 nM BIO, and 40 ng/ml Wnt3a. *D,* migration assay of podocytes following PBS, lithium, TDZD, or BIO treatment for 24 h. Representative pictures are shown. *E,* number of cells migrated were quantified, and the results are shown as the mean ± S.D. of three independent experiments. *, $p < 0.05$.

increase in urinary Wt1 levels in 6- and 7-week-old heterozygous and homozygous mice. The increase in urinary Wt1 level preceded the development of albuminuria (Fig. 3*M*).

Gene expression analysis also indicated a decrease of glomerular Itgb1 mRNA levels, which was evident in NPHS2^{Cre}/Ctnnb1$^{FloxE3/WT}$ mice and even more pronounced in NPHS2^{Cre}/Ctnnb1$^{FloxE3/FloxE3}$ mice (Fig. 3*K*). In wild type mice, active Itgb1 was localized to mesangial cells and podocytes, whereas Itga3 expression was mostly restricted to podocytes (supplemental Fig. S3*A*). In NPHS2^{Cre}/Ctnnb1$^{FloxE3/FloxE3}$ mice, there was a decrease in Itgb1 expression in podocytes, and therefore, there was less of an overlap between Itga3 and Itgb1 expression. Integrin-linked kinase (Ilk) expression was mainly restricted to podocytes in control animals, and its expression was significantly decreased in NPHS2^{Cre}/Ctnnb1$^{FloxE3/FloxE3}$ mice (supplemental Fig. S3*B*). These results suggest that decreased integrin and Ilk expression might be responsible for urinary podocyte loss, which preceded albuminuria development and glomerular podocyte loss.

Wnt/Ctnnb1 Activation in Vitro in Podocytes Leads to Decreased Adhesion—To examine the downstream targets of Ctnnb1 in podocytes, we generated podocyte cell lines with stabilized Ctnnb1 using Immorto/Ctnnb1$^{FloxE3/FloxE3}$ mice (30, 37). Podocyte clones ($n = 7$) were established by serial dilution and selected based on their expression of podocyte-specific markers (*Nphs1*, *Nphs2*, *Synpo*, and *Wt1*). Consistent with prior reports, cells expressed only low levels (mRNA) of *Nphs1* upon differentiation (*Nphs2* and *Wt1* expression was high). To induce Cre-mediated recombination, podocytes were infected with Cre or control adenoviruses. Western blot analysis for Ctnnb1 showed the presence of a truncated ΔExon3-Ctnnb1 expression following Cre infection (Fig. 4*A*). Immunocytochemistry showed nuclear accumulation of Ctnnb1 in Immorto/Ctnnb1$^{FloxE3/FloxE3}$ podocytes (Fig. 4*B*). Furthermore, following Cre infection, a significant increase in classic Ctnnb1 target gene expression, including *Axin2*, *Tcf7*, and *Cd44*, was observed, indicating transcriptional activation of Ctnnb1 (Fig. 4*C*). Expression of podocyte differentiation genes (*Nphs1, Nphs2, Synpo,* and *Wt1*) were not significantly altered following Cre infection (Fig. 4*D*) nor transcript levels of apoptosis-related genes (Cdkn1a, *Tp53, Bax,* and *Apaf1*) (Fig. 4*E*). Protein expression of cleaved poly(ADP-ribose) polymerase and Cdkn1a was slightly lower in cells after Ctnnb1 activation (Fig. 4*F*).

Two independent clones of Ctnnb1$^{FloxE3/FloxE3}$ podocytes showed significantly lower adhesiveness to type IV collagen compared with the same clone with control adenoviral infection (Fig. 4*G*). Gene expression studies of podocyte clones with Ctnnb1 activation showed lower expression of *Col4a3* and *Col4a4* (podocyte-specific collagen) and *Mmp16* and *Mmp23* (Fig. 4, *H* and *I*). In addition, we observed a significant decrease in Itgb1 expression following Cre recombination (Fig. 4*F*). Total Ilk or Fak levels did not change significantly (Fig. 4*F*), although phospho-Fak$^{Tyr\text{-}397}$ was lower following Cre recombination. These results suggest that active Ctnnb1 expression was associated with decreased adhesiveness in podocytes, which could be due to the decrease in Itgb1 expression and focal adhesion kinase (FAK) phosphorylation (38).

We also examined whether canonical Wnt ligand treatment leads to a similar phenotype. Recombinant Wnt3a treatment

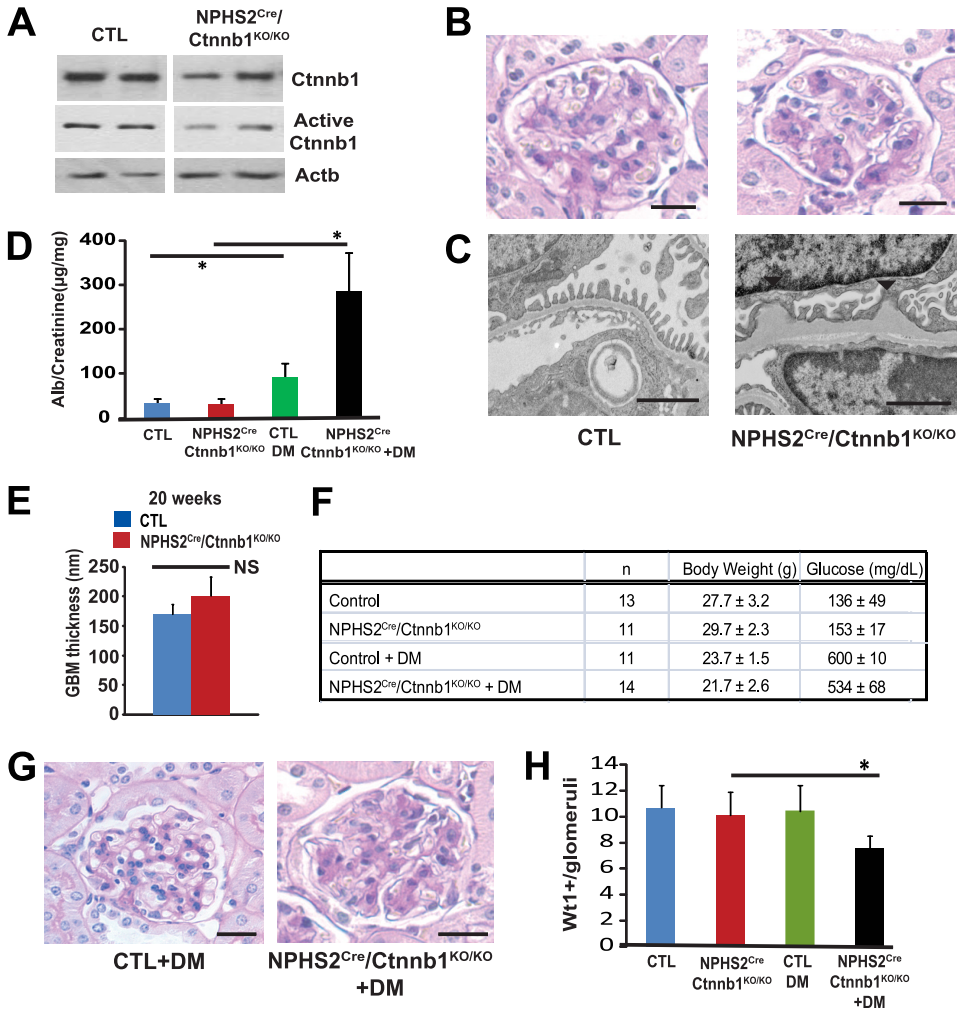

	n	Body Weight (g)	Glucose (mg/dL)
Control	13	27.7 ± 3.2	136 ± 49
NPHS2^{Cre}/Ctnnb1$^{KO/KO}$	11	29.7 ± 2.3	153 ± 17
Control + DM	11	23.7 ± 1.5	600 ± 10
NPHS2^{Cre}/Ctnnb1$^{KO/KO}$ + DM	14	21.7 ± 2.6	534 ± 68

FIGURE 6. **Podocyte-specific Ctnnb1 knock-out mice show increased susceptibility to diabetic kidney injury.** *A*, total and active Ctnnb1 and Actb Western blot analysis of isolated glomeruli of control (*CTL*) and NPHS2^{Cre}/Ctnnb1$^{KO/KO}$ mice. *B*, PAS-stained or TEM (*C*) kidney sections of 20-week-old male control and NPHS2^{Cre}/Ctnnb1$^{KO/KO}$ mice. PAS *scale bar*, 20 μm. TEM *scale bar*, 2 μm. *Arrowheads* indicate the splittings of GBM (*C*). *D*, urinary albumin-to-creatinine ratios of 20-week-old male control (*blue bar*), NPHS2^{Cre}/Ctnnb1$^{KO/KO}$, diabetic control, and diabetic NPHS2^{Cre}/Ctnnb1$^{KO/KO}$ mice. *, $p < 0.05$. *E*, quantification of basement membrane thickness of 20-week-old male control and NPHS2^{Cre}/Ctnnb1$^{KO/KO}$ mice. *F*, body weight and blood glucose levels of control, control diabetic, NPHS2^{Cre}/Ctnnb1$^{KO/KO}$, and diabetic NPHS2^{Cre}/Ctnnb1$^{KO/KO}$ mice. *G*, PAS-stained kidney sections of 20-week-old male control diabetic and diabetic NPHS2^{Cre}/Ctnnb1$^{KO/KO}$ mice. *H*, Wt1 positive cell number/glomerulus of 20-week-old male control (*blue bar*), NPHS2^{Cre}/Ctnnb1$^{KO/KO}$ (*red*), diabetic control (*green*), and diabetic NPHS2^{Cre}/Ctnnb1$^{KO/KO}$ (*black*) mice. *, $p < 0.05$.

increased active Ctnnb1 levels, without significantly affecting total Ctnnb1 levels (Fig. 5*A*). Immunofluorescence studies showed nuclear accumulation of Ctnnb1 following Wnt3a treatment (Fig. 5*B*). These results indicate that cultured podocytes respond to Wnt signaling. Podocytes treated with Wnt3a or different GSK3β inhibitors, LiCl, BIO, and TDZD-8, were less adhesive to type I and type IV collagens and laminin (Fig. 5*C*). Treatment with GSK3β inhibitors also significantly lowered cell motility compared with control PBS (Fig. 5, *D* and *E*). These results suggest that Wnt/Ctnnb1 activation in podocytes is associated with decreased adhesiveness and migration.

Podocyte-specific Ctnnb1 Knock-out Mice and Mice with Podocyte-specific Dkk1 Overexpression Show Minor GBM Alterations and Increased Susceptibility to Diabetic Kidney Injury—To further understand the role of Ctnnb1, we generated mice with podocyte-specific Ctnnb1 deletion by crossing NPHS2^{Cre} mice with Ctnnb1$^{KO/KO}$ mice. Total and active Ctnnb1 expression was reduced in glomerular lysates of NPHS2^{Cre}/Ctnnb1$^{KO/KO}$ mice (Fig. 6*A*). Kidney histology of the NPHS2^{Cre}/Ctnnb1$^{KO/KO}$ mice appeared normal (Fig. 6*B*), and mice did not show signs of albuminuria even at 20 weeks of age (Fig. 6*D*). Electron microscopic analysis indicated minor GBM alterations, evident mainly as occasional GBM splitting (Fig. 6*C*). Quantitative analysis of GBM width, however, did not reveal statistically significant differences in overall GBM thickness (Fig. 6*E*).

As we observed increased activation of the Wnt/Ctnnb1 pathway in DKD glomeruli, we wanted to determine the role of the Wnt/Ctnnb1 pathway in DKD. Diabetes was induced by low dose STZ injection in uninephrectomized male mice at 5 weeks of age. Control and podocyte-specific Ctnnb1 knock-out mice showed similar body weight and degree of hyperglycemia at 20 weeks of age (Fig. 6*F*), when they were sacrificed. Control diabetic mice had only a minimal increase in albuminuria compared with nondiabetic mice (Fig. 6*D*). However, diabetic NPHS2^{Cre}/Ctnnb1$^{KO/KO}$ mice at 20 weeks of age exhibited sig-

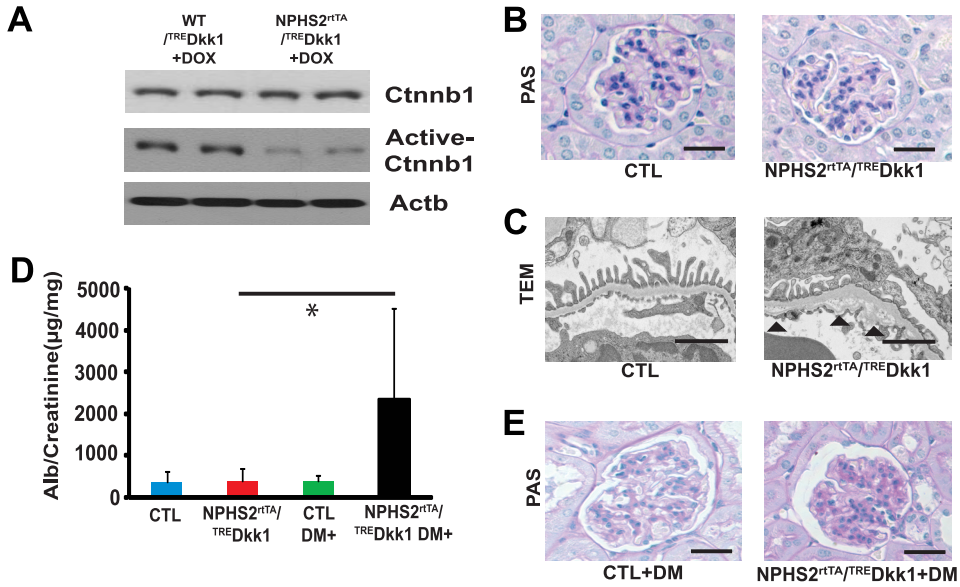

FIGURE 7. **Podocyte-specific Dkk1 transgenic mice recapitulate the phenotypes of Ctnnb1 knock-out mice.** *A,* Western blot analysis of total and active Ctnnb1 and Actb of isolated glomeruli of 20-week-old control (*CTL*; WT/^{TRE}Dkk1) and NPHS2^{rtTA}/^{TRE}Dkk1 lysates. Mice were fed with doxycycline-containing food for 17 weeks from 3 weeks of age. *B,* PAS-stained kidney sections and TEM analysis (*C*) of 20-week-old male control and NPHS2^{rtTA}/^{TRE}Dkk1 mice fed with doxycycline-containing food for 17 weeks. *Scale bar,* 20 μm (*B*) and 2 μm (*C*). *Arrowheads* indicate the splittings of GBM (*C*). *D,* albumin-to-creatinine ratios of 20-week-old male control (*blue*), NPHS2^{rtTA}/^{TRE}Dkk1 (*red*), diabetic control (*green*), and diabetic NPHS2^{rtTA}/^{TRE}Dkk1 mice (*black*) ($n = 9–17$ per group). *, $p < 0.05$. *E,* PAS-stained kidney sections of control diabetic (*CTL+DM*) and diabetic NPHS2^{rtTA}/^{TRE}Dkk1 mice fed with doxycycline-containing food for 17 weeks.

nificantly increased albuminuria and mesangial expansion compared with control diabetic mice (Fig. 6, *D* and *G*). In addition, significantly greater podocyte loss was detected in NPHS2^{Cre}/Ctnnb1$^{KO/KO}$ diabetic mice when compared with control diabetic mice (Fig. 6*H*), and there was a greater decrease in nephrin and podocin staining. These studies indicate increased susceptibility to podocyte loss and DKD in NPHS2^{Cre}/Ctnnb1$^{KO/KO}$ diabetic animals.

To differentiate between the two key roles of Ctnnb1 (cell adhesion and Wnt signaling) and to avoid the potential impact of Ctnnb1 on kidney development, we generated mice with podocyte-specific inducible Dickkopf-related protein 1 (Dkk1) transgenic mice (NPHS2^{rtTA}/^{TRE}-Dkk1) (26). Dkk1 is a secreted Wnt antagonist, capable of blocking Wnt binding to LRP5/6 co-receptors, thus inhibiting canonical Wnt/Ctnnb1 signaling (39). We induced Dkk1 expression by feeding mice with doxycycline-containing food starting at 3 weeks of age. Active Ctnnb1 protein expression was reduced in glomerular lysates of NPHS2^{rtTA}/^{TRE}-Dkk1 mice, although total Ctnnb1 levels were not changed (Fig. 7*A*). These results suggest the presence of base line Wnt-dependent signaling in the glomerulus/podocytes. At base line, NPHS2^{rtTA}/^{TRE}-Dkk1 mice showed neither apparent light microscopic abnormalities nor albuminuria (Fig. 7, *B* and *D*). Transmission EM analysis showed occasional GBM splitting, similar to that observed in NPHS2^{Cre}/Ctnnb1$^{KO/KO}$ mice (Fig. 7*C*).

Next, we studied the effect of diabetes in uninephrectomized male mice following low dose STZ injection. At 20 weeks of age, diabetic NPHS2^{rtTA}/^{TRE}-Dkk1 mice had significantly increased albuminuria and glomerulosclerosis compared with control diabetic mice (Fig. 7, *D* and *E*). These changes were similar to those observed in NPHS2^{Cre}/Ctnnb1$^{KO/KO}$ mice. These results suggest that inhibiting podocyte Wnt signaling in the context of diabetes is deleterious.

Ctnnb1 Deletion from Podocytes Promotes Cell Differentiation and Adhesion but Increases Apoptosis Susceptibility—We generated multiple podocyte clones with Ctnnb1 deletion using the Immorto/Ctnnb1$^{KO/KO}$ mice. The successful deletion of Ctnnb1 was confirmed by QRT-PCR (QRT-PCR data is not shown), Ctnnb1 Western blots, and by immunofluorescence studies (Fig. 8, *A* and *B*). Podocytes with Ctnnb1 deletion showed decreased expression of the Ctnnb1 target gene *Axin2*, indicating a potential base-line transcriptional activity of Ctnnb1 in cultured podocytes (Fig. 8*C*). Ctnnb1 deletion did not induce significant changes in collagen and slightly increased Mmp2 expression (Fig. 8, *D* and *E*). Podocytes clones showed a mild but statistically significant increased expression of differentiated podocyte markers, including *Wt1* and *Nphs2* after Ctnnb1 silencing (Fig. 8*F*). Consistent with these findings, mRNA levels of podocyte-specific genes, including *Wt1, Nphs1, Plce1, Pdxl,* and *Synpo*, were slightly but significantly increased in podocyte-specific Ctnnb1 knock-out animals as compared with control mice (supplemental Table 2).

Ctnnb1$^{KO/KO}$ podocytes showed increased adhesiveness to type IV collagen (Fig. 8*G*). In addition, there was a minor but consistent increase in phospho-Fak levels following Cre infection, although total Ilk and total Fak levels were unchanged (Fig. 8*H*).

Further analysis indicated that cells with Ctnnb1 deletion had increased mRNA levels of *Cdkn1a*, *Tp53*, and *Apaf1* (Fig. 8*I*). Protein expression of Cdkn1a and phosphorylated p53 were significantly increased following Ctnnb1 deletion (Fig. 8*H*). Moreover, the increase in cleaved poly(ADP-ribose) polymerase levels following Ctnnb1 deletion confirmed the increased apoptotic rate (Fig. 8*H*). In summary, podocyte-specific Ctnnb1 deletion *in vitro* was associated with increased expression of differentiation markers of podocyte (Wt1 and Nphs2) and

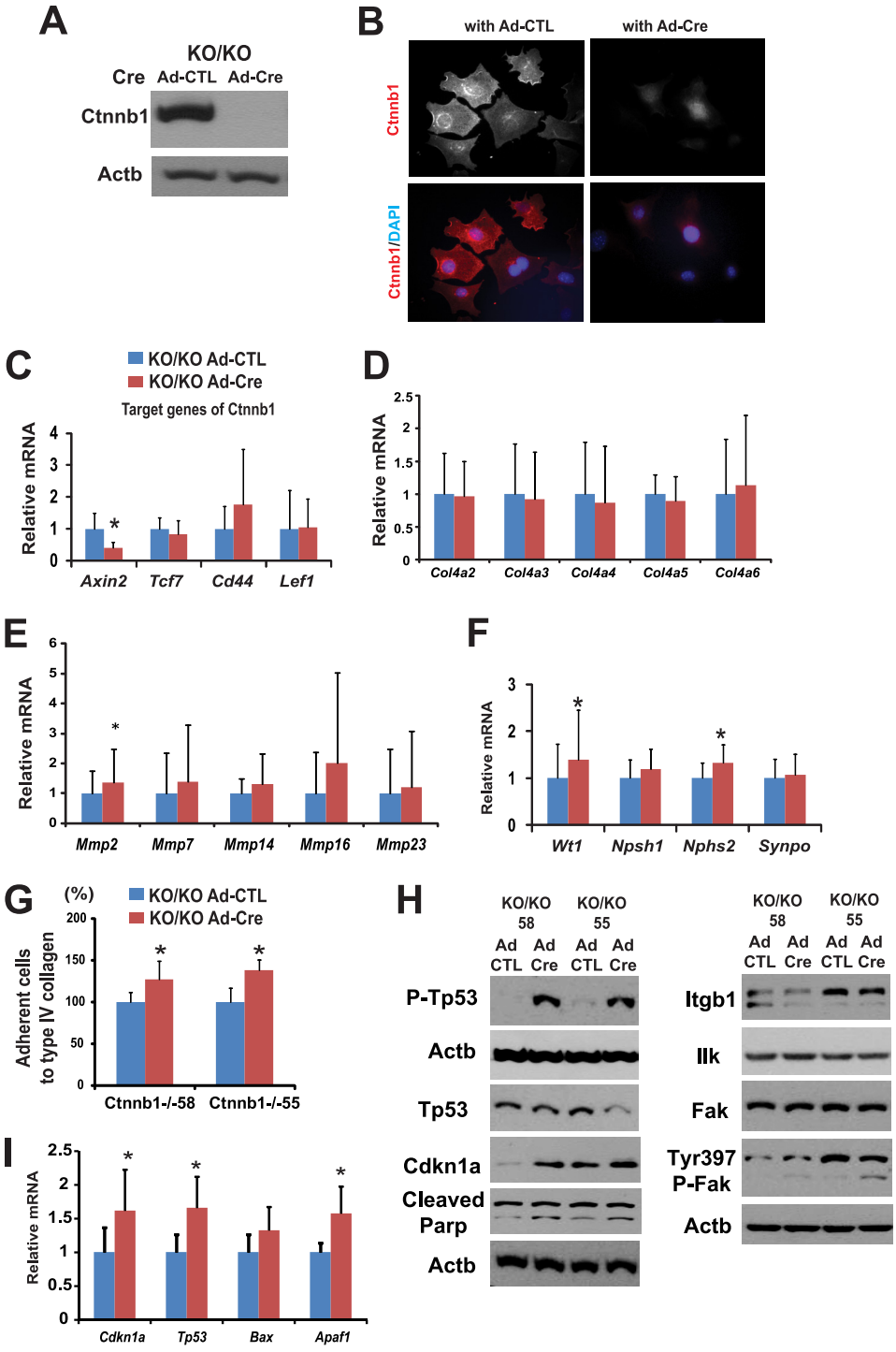

FIGURE 8. **Loss of Ctnnb1 in cultured podocytes increased adhesiveness, differentiation markers, and susceptibility to apoptosis.** *A,* Western blot for Ctnnb1 of Immorto/Ctnnb1$^{KO/KO}$ podocyte clones (labeled as *KO/KO*) 4 days after control or Cre adenoviral infection. *B,* total Ctnnb1 (*red*) immunocytochemistry of Ctnnb1$^{KO/KO}$ podocytes infected with control (*left*) or Cre adenovirus (*right*). DAPI (*blue*), nuclear counterstaining. *C–F* and *I*, QRT-PCR and Western blot (*F*) analysis of Immorto/Ctnnb1$^{KO/KO}$ clones (KO/KO) infected with control or Cre adenovirus. QRT-PCR data are expressed as mean fold change ± S.D. Paired *t* test was used for QRT-PCR, *, $p < 0.05$. *G,* cell adhesion to type IV collagen using the Vybant adhesion assay of two independent Ctnnb1$^{KO/KO}$ podocytes clones. The percentage adhesion was calculated relative to that of control adenovirus. *H,* Western blot analysis of Immorto/Ctnnb1$^{KO/KO}$ clones infected with control or Cre adenovirus *, $p < 0.05$.

increased adhesiveness; however, these cells appeared to be more susceptible to apoptosis.

DISCUSSION

Here, we investigated the physiological and pathological role of the Wnt/Ctnnb1 pathway specifically in podocytes. Our experiments were prompted by genome-wide association studies showing an association between TCF7L2 polymorphism (a key transcription factor in the Wnt/Ctnnb1 signaling pathway) and diabetes and DKD development (15). Here, we show the activation of Wnt/Ctnnb1 signaling in human and rodent diabetic models. Our previous genome-wide transcript analysis

study identified five key pathways with differential regulation in glomeruli isolated from patients with advanced DKD. They were Wnt/Ctnnb1, integrin, RhoA, macropinocytosis, and complement pathways (17). These results indicate a strong potential consensus on the activation of the Wnt/Ctnnb1 signaling in diabetic podocytes and glomeruli.

We and others have identified hyperglycemia-induced podocyte apoptosis as an early lesion in diabetic glomeruli (40). In some organs, the activation of the Wnt/Ctnnb1 pathway is observed following apoptosis or injury, and it could contribute to organ regeneration. The Wnt/Ctnnb1 pathway is regarded as a strong pro-survival signal; therefore, Wnt pathway activation might represent a survival signal in DKD podocytes. Interestingly, after the initial wave of apoptosis, podocyte apoptosis rate is much lower (almost absent) in diabetic animal models, indicating that cells either become resistant to apoptosis or activate survival signals.

We found that mice with podocyte-specific expression of stabilized Ctnnb1 ($NPHS2^{Cre}/Ctnnb1^{FloxE3/WT}$) presented with basement membrane thickening and albuminuria, a phenotype similar to early human DKD. These results could indicate that increased activity of Wnt/Ctnnb1 might play a causal role in DKD development. Detailed analyses of these mice and cultured podocytes indicated that the Wnt/Ctnnb1 pathway activation might present with some minor survival benefits, as there was a minor decrease in cleaved poly(ADP-ribose) polymerase levels in cultured knock-out cells (40). However, the effect of Ctnnb1 activation on loss of differentiation markers and cell adhesiveness was much greater. Similar to other cell types, the Wnt/Ctnnb1 pathway in podocytes appears to interact with integrin and focal adhesion kinase signaling pathways (41). The overall effect of Wnt/Ctnnb1 activation was podocyte detachment and the development of albuminuria. This phenotype (GBM thickening followed by albuminuria) was similar to the podocyte-specific *Ilk*, *Ddr1*, *Itgb1*, and *Itga3* knock-out animals (11, 12, 28), indicating that these genes most likely lie on the same pathway.

Mice with podocyte-specific Ctnnb1 deletion and podocyte-specific expression of Wnt inhibitor Dkk1 (Ctnnb1 KO and Dkk1 transgenic mice) showed similar base-line phenotype, minor GBM abnormalities, evident as occasional splitting of the GBM. Moreover, we observed decreased expression of the Ctnnb1 target gene *Axin2* after Ctnnb1 deletion or inhibition. These results indicate that low level Wnt/Ctnnb1 signaling might still be active in podocytes. Furthermore, cultured podocytes with Ctnnb1 deletion showed increased expression of podocyte differentiation markers *Wt1* and *Nphs2 in vitro* and *Wt1, Nphs1, Pdxl,* and *Synpo in vivo*. These results indicate that decreasing podocyte Wnt/Ctnnb1 might be necessary for full podocyte differentiation. We have very little knowledge regarding how to enhance podocyte differentiation; therefore, these results might open new avenues for further investigations.

Despite that loss of Ctnnb1 enhanced podocyte adhesiveness and differentiation, the absence of Ctnnb1 in podocytes enhanced susceptibility to DKD. Moreover, we also show that this is related to inhibition of canonical Wnt signaling, as mice with podocyte-specific expression of Dkk1 phenocopied the $NPHS^{cre}/Ctnnb1^{KO/KO}$ mice. Interestingly, the phenotype of

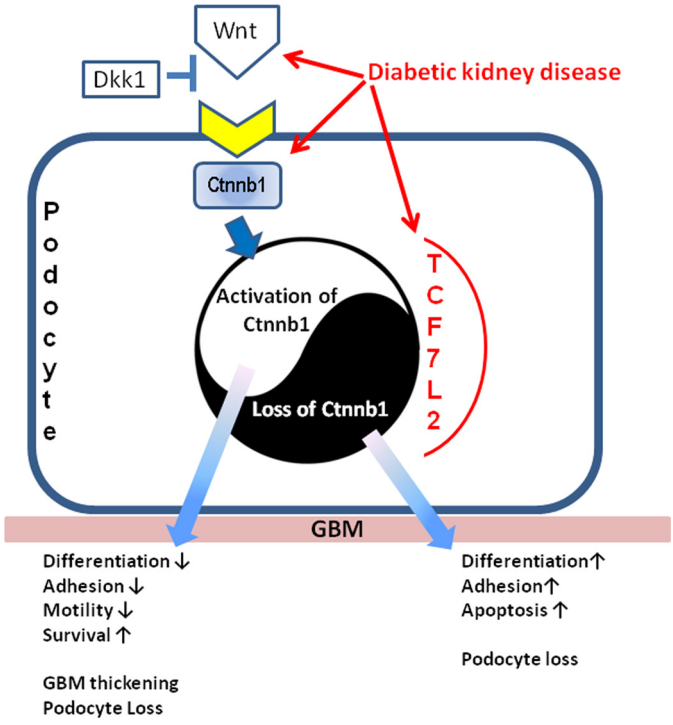

FIGURE 9. **Summary.** Our results indicate that the Wnt/Ctnnb1 pathway plays a key role in podocyte adhesion, motility, differentiation, and survival. Increased activation of the pathway in DKD might occur to promote podocyte survival, but it also leads to cell detachment and podocyte loss. Down-regulation of the Wnt/Ctnnb1 pathway in podocytes might be important for terminal differentiation; however, it enhances apoptosis susceptibility.

diabetic $NPHS^{rtTA}/^{TRE}Dkk1$ animals was more severe than diabetic $NPHS^{cre}/Ctnnb1^{KO/KO}$ mice. This observation could be consistent with the issue that Ctnnb1 deletion would only inhibit autonomous Wnt signaling, although Dkk1 expression could also inhibit Wnt signaling in neighboring cells. Ctnnb1 loss *in vitro* enhanced podocyte susceptibility to apoptosis, which was most likely responsible for the enhanced DKD susceptibility of these animals. This is in line with previous reports that Tp53 expression was necessary for terminal differentiation of the renal epithelium; however, Tp53 is also a key regulator of apoptosis. The finding that podocyte-specific Ctnnb1 knock-out mice are more susceptible to injury is different from prior publications showing that these mice were less susceptible to adriamycin nephropathy (18, 42). These fundamental differences might be related to the type and length of injury induced by diabetes (15 weeks) *versus* the acute model caused by high dose adriamycin injection (4 days). Upon analysis of the short term and non-nephrotic range albuminuria (induced by LPS injection), podocyte-specific Ctnnb1 knock-out mice exhibited a similar degree of albuminuria (or even less) to control mice (supplemental Fig. S4). Other key differences are related to the mechanism of Ctnnb1-induced changes in podocytes. Previously, it has been proposed that Ctnnb1 would down-regulate nephrin expression via the transcription factor Snail. Our *in vivo* and *in vitro* studies did not show Ctnnb1-induced regulation of Snail (supplemental Fig. S5). Moreover, the slow time course of albuminuria development in the $NPHS2^{Cre}/Ctnnb1^{FloxE3}$ would not be consistent with this model.

In summary, our results indicate that the Wnt/Ctnnb1 pathway plays a key role in podocyte adhesion, motility, differentiation, and survival. Increased activation of the pathway in DKD might occur to promote podocyte survival, but it also leads to cell detachment and podocyte loss. Down-regulation of the Wnt/Ctnnb1 pathway in podocytes might be important for terminal differentiation; however, it enhances apoptosis susceptibility (Fig. 9). These studies illustrate the relationship between cell differentiation, adhesion, and cell death and demonstrate why podocytes are so prone to injury. Recognizing the role of Wnt/Ctnnb1 can help us to understand DKD development.

Acknowledgments—We thank Jeffrey B. Kopp (NIDDK, National Institutes of Health) for providing us with the NPHS2^{rtTA} mice and Roya Shaji for critical reading of the manuscript. We also thank Dr. Fuad Spath for his help.

REFERENCES

1. Foley, R. N., and Collins, A. J. (2007) *J. Am. Soc. Nephrol.* **18,** 2644–2648
2. Miner, J. H., and Sanes, J. R. (1996) *J. Cell Biol.* **135,** 1403–1413
3. Kaplan, J. M., Kim, S. H., North, K. N., Rennke, H., Correia, L. A., Tong, H. Q., Mathis, B. J., Rodríguez-Pérez, J. C., Allen, P. G., Beggs, A. H., and Pollak, M. R. (2000) *Nat. Genet.* **24,** 251–256
4. Faul, C., Asanuma, K., Yanagida-Asanuma, E., Kim, K., and Mundel, P. (2007) *Trends Cell Biol.* **17,** 428–437
5. Pagtalunan, M. E., Miller, P. L., Jumping-Eagle, S., Nelson, R. G., Myers, B. D., Rennke, H. G., Coplon, N. S., Sun, L., and Meyer, T. W. (1997) *J. Clin. Invest.* **99,** 342–348
6. Susztak, K., Raff, A. C., Schiffer, M., and Böttinger, E. P. (2006) *Diabetes* **55,** 225–233
7. Yu, D., Petermann, A., Kunter, U., Rong, S., Shankland, S. J., and Floege, J. (2005) *J. Am. Soc. Nephrol.* **16,** 1733–1741
8. Wiggins, R. C. (2007) *Kidney Int.* **71,** 1205–1214
9. Kriz, W., Gretz, N., and Lemley, K. V. (1998) *Kidney Int.* **54,** 687–697
10. Niranjan, T., Bielesz, B., Gruenwald, A., Ponda, M. P., Kopp, J. B., Thomas, D. B., and Susztak, K. (2008) *Nat. Med.* **14,** 290–298
11. Kreidberg, J. A., Donovan, M. J., Goldstein, S. L., Rennke, H., Shepherd, K., Jones, R. C., and Jaenisch, R. (1996) *Development* **122,** 3537–3547
12. Pozzi, A., Jarad, G., Moeckel, G. W., Coffa, S., Zhang, X., Gewin, L., Eremina, V., Hudson, B. G., Borza, D. B., Harris, R. C., Holzman, L. B., Phillips, C. L., Fassler, R., Quaggin, S. E., Miner, J. H., and Zent, R. (2008) *Dev. Biol.* **316,** 288–301
13. Moon, R. T., Kohn, A. D., De Ferrari, G. V., and Kaykas, A. (2004) *Nat. Rev. Genet.* **5,** 691–701
14. Willert, K., and Jones, K. A. (2006) *Genes Dev.* **20,** 1394–1404
15. Köttgen, A., Hwang, S. J., Rampersaud, E., Coresh, J., North, K. E., Pankow, J. S., Meigs, J. B., Florez, J. C., Parsa, A., Levy, D., Boerwinkle, E., Shuldiner, A. R., Fox, C. S., and Kao, W. H. (2008) *J. Am. Soc. Nephrol.* **19,** 1989–1999
16. Sale, M. M., Smith, S. G., Mychaleckyj, J. C., Keene, K. L., Langefeld, C. D., Leak, T. S., Hicks, P. J., Bowden, D. W., Rich, S. S., and Freedman, B. I. (2007) *Diabetes* **56,** 2638–2642
17. Cohen, C. D., Lindenmeyer, M. T., Eichinger, F., Hahn, A., Seifert, M., Moll, A. G., Schmid, H., Kiss, E., Gröne, E., Gröne, H. J., Kretzler, M., Werner, T., and Nelson, P. J. (2008) *PLoS ONE* **3,** e2937
18. Dai, C., Stolz, D. B., Kiss, L. P., Monga, S. P., Holzman, L. B., and Liu, Y. (2009) *J. Am. Soc. Nephrol.* **20,** 1997–2008
19. Lin, C. L., Wang, J. Y., Huang, Y. T., Kuo, Y. H., Surendran, K., and Wang, F. S. (2006) *J. Am. Soc. Nephrol.* **17,** 2812–2820
20. Lin, C. L., Wang, J. Y., Ko, J. Y., Huang, Y. T., Kuo, Y. H., and Wang, F. S. (2010) *J. Am. Soc. Nephrol.* **21,** 124–135
21. Si, H., Banga, R. S., Kapitsinou, P., Ramaiah, M., Lawrence, J., Kambhampati, G., Gruenwald, A., Bottinger, E., Glicklich, D., Tellis, V., Greenstein, S., Thomas, D. B., Pullman, J., Fazzari, M., and Susztak, K. (2009) *PLoS One* **4,** e4802
22. Takemoto, M., He, L., Norlin, J., Patrakka, J., Xiao, Z., Petrova, T., Bondjers, C., Asp, J., Wallgard, E., Sun, Y., Samuelsson, T., Mostad, P., Lundin, S., Miura, N., Sado, Y., Alitalo, K., Quaggin, S. E., Tryggvason, K., and Betsholtz, C. (2006) *EMBO J.* **25,** 1160–1174
23. Harada, N., Tamai, Y., Ishikawa, T., Sauer, B., Takaku, K., Oshima, M., and Taketo, M. M. (1999) *EMBO J.* **18,** 5931–5942
24. Moeller, M. J., Sanden, S. K., Soofi, A., Wiggins, R. C., and Holzman, L. B. (2002) *J. Am. Soc. Nephrol.* **13,** 1561–1567
25. Brault, V., Moore, R., Kutsch, S., Ishibashi, M., Rowitch, D. H., McMahon, A. P., Sommer, L., Boussadia, O., and Kemler, R. (2001) *Development* **128,** 1253–1264
26. Shigehara, T., Zaragoza, C., Kitiyakara, C., Takahashi, H., Lu, H., Moeller, M., Holzman, L. B., and Kopp, J. B. (2003) *J. Am. Soc. Nephrol.* **14,** 1998–2003
27. Chu, E. Y., Hens, J., Andl, T., Kairo, A., Yamaguchi, T. P., Brisken, C., Glick, A., Wysolmerski, J. J., and Millar, S. E. (2004) *Development* **131,** 4819–4829
28. El-Aouni, C., Herbach, N., Blattner, S. M., Henger, A., Rastaldi, M. P., Jarad, G., Miner, J. H., Moeller, M. J., St-Arnaud, R., Dedhar, S., Holzman, L. B., Wanke, R., and Kretzler, M. (2006) *J. Am. Soc. Nephrol.* **17,** 1334–1344
29. Harvey, S. J., and Miner, J. H. (2008) *Curr. Opin. Nephrol. Hypertens.* **17,** 393–398
30. Mundel, P., Reiser, J., Zúñiga Mejía Borja, A., Pavenstädt, H., Davidson, G. R., Kriz, W., and Zeller, R. (1997) *Exp. Cell Res.* **236,** 248–258
31. Lorenzen, J., Shah, R., Biser, A., Staicu, S. A., Niranjan, T., Garcia, A. M., Gruenwald, A., Thomas, D. B., Shatat, I. F., Supe, K., Woroniecki, R. P., and Susztak, K. (2008) *J. Am. Soc. Nephrol.* **19,** 884–890
32. Dandapani, S. V., Sugimoto, H., Matthews, B. D., Kolb, R. J., Sinha, S., Gerszten, R. E., Zhou, J., Ingber, D. E., Kalluri, R., and Pollak, M. R. (2007) *J. Biol. Chem.* **282,** 467–477
33. Brosius, F. C., 3rd, Alpers, C. E., Bottinger, E. P., Breyer, M. D., Coffman, T. M., Gurley, S. B., Harris, R. C., Kakoki, M., Kretzler, M., Leiter, E. H., Levi, M., McIndoe, R. A., Sharma, K., Smithies, O., Susztak, K., Takahashi, N., and Takahashi, T. (2009) *J. Am. Soc. Nephrol.* **20,** 2503–2512
34. Miner, J. H. (1998) *Curr. Opin. Nephrol. Hypertens.* **7,** 13–19
35. Jefferson, J. A., Shankland, S. J., and Pichler, R. H. (2008) *Kidney Int.* **74,** 22–36
36. Susztak, K., Böttinger, E., Novetsky, A., Liang, D., Zhu, Y., Ciccone, E., Wu, D., Dunn, S., McCue, P., and Sharma, K. (2004) *Diabetes* **53,** 784–794
37. Shankland, S. J., Pippin, J. W., Reiser, J., and Mundel, P. (2007) *Kidney Int.* **72,** 26–36
38. Ma, H., Togawa, A., Soda, K., Zhang, J., Lee, S., Ma, M., Yu, Z., Ardito, T., Czyzyk, J., Diggs, L., Joly, D., Hatakeyama, S., Kawahara, E., Holzman, L., Guan, J. L., and Ishibe, S. (2010) *J. Am. Soc. Nephrol.* **21,** 1145–1156
39. Zorn, A. M. (2001) *Curr. Biol.* **11,** R592–R595
40. Szabó, C., Biser, A., Benko, R., Böttinger, E., and Suszták, K. (2006) *Diabetes* **55,** 3004–3012
41. Ashton, G. H., Morton, J. P., Myant, K., Phesse, T. J., Ridgway, R. A., Marsh, V., Wilkins, J. A., Athineos, D., Muncan, V., Kemp, R., Neufeld, K., Clevers, H., Brunton, V., Winton, D. J., Wang, X., Sears, R. C., Clarke, A. R., Frame, M. C., and Sansom, O. J. (2010) *Dev. Cell* **19,** 259–269
42. Heikkilä, E., Juhila, J., Lassila, M., Messing, M., Perälä, N., Lehtonen, E., Lehtonen, S., Sjef Verbeek, J., and Holthofer, H. (2010) *Nephrol. Dial. Transplant.* **25,** 2437–2446